

Feature Selection from 3D Brain Model for Some Dementia Subtypes Using Genetic Algorithm

Savaş Okay¹, Nihat Adar^{*1}, Kemal Özkan¹, Baki Adapınar²

Accepted : 11/07/2017 Published: 31/07/2017

Abstract: Brain scans that are appropriate to the medical standards are obtained from magnetic resonance imaging devices. Through image processing techniques, 3D brain models can be constructed by mapping medical brain imaging files structurally. Physical characteristics of patient brains can be extracted from those 3D brain models. Characteristics of some specific brain regions are more efficacious in predicting the type of the disease. For that reason, researches are made for finding the worthwhile features out using cortical volumes, gray volumes, surface areas, and thickness averages for left and right brain parts separately or together. The main objective of this work is determining more influential sections throughout the entire brain in establishing the clinical diagnosis. To that end, among all the measurements exported from 3D models, the significant brain features that are effective in identifying some dementia subtypes are sought. The dataset has 3D brain models generated from magnetic resonance scans of 63 samples. Each sample is labeled with one of the following three disease types: Alzheimer's disease (19), frontotemporal dementia (19), and vascular dementia (25). The genetic algorithm based wrapper feature selection method with various classifiers is proposed to select the features that state the aforementioned dementia subtypes best. The tests are performed by applying cross validation technique and confusion matrices are shown. At the end, the best features are listed, and the accuracy results up to 95.2% are achieved.

Keywords: 3D brain model, Dementia subtypes, Feature selection, Genetic algorithm, Magnetic resonance imaging

1. Introduction

Dementias are entitled as neuropsychiatric disorders. As people get older, the rate of occurrence of these abnormalities also increases. Such diseases are related to loss of mental functions, cognitive impairments, and sometimes variations in personality [1]. The most frequently encountered subtypes of dementia are Alzheimer's disease (AD), vascular dementia (VaD), and frontotemporal dementia (FTD) respectively. According to the statistical report of a research conducted in 2003, it was estimated that the number of demented elderly people worldwide could see 63 million in 2030, and 114 million in 2050 [2].

During the medical tests, specific brain regions over patients' brain scans are observed for clinical identification. These scans are obtained from imaging studies with magnetic resonance imaging (MRI) devices. MRI is a technique for understanding of the body anatomy with the help of radio waves and the use of magnets, and it does not contain radiation. One of the sequences used in this technique is T1 sequence. Soft tissue contrast is acquired more conveniently in T1 sequenced images [3].

There are many different MRI systems. Therefore, procedures or outputs may differ from device to device. Such situations must be taken into consideration in advance. After imaging studies being produced, output files appropriate to the medical imaging

standards are procured from MRI systems. These output files usually have a definite file extension namely *digital imaging and communications in medicine* (dicom), and they are in 2D sliced form which represents the projection of the brain to different axes. Each of these dicom files contains technical or non-technical information besides the sliced image. Desired information of a particular patient can be reached by reading the header part of the dicom file, or by processing the visual part of the same file with the use of image processing techniques. 3D brain models can be constructed by mapping those files structurally. After extracting features from 3D model data, classification of the unidentified disease may be carried out using those values. While the classification operations are being performed, it is possible that some of the features are more precious than the others. Thereby, it is important to select the valuable attribute subset rather than the whole set as input, in order to make the classification prediction more accurate. In this regard, intuitive feature selection algorithms that are not behaving like brute force methods, have been developed to find the best possible subset of attributes. In the wrapper feature selection methods, it is aimed to reach the best set of attributes by considering the classification results belonging to the selected set [4].

Many important studies have been made in the field of brain imaging within interdisciplinary studies between medical and computer sciences in recent years. There are numerous researches using free standard datasets such as Alzheimer's Disease Neuroimaging Initiative (ADNI), AddNeuroMed, etc. Even more, a wide range of researches uses their own dataset. In computer-assisted studies, some software tools are operated to extract features from brain scans. The Freesurfer brain analyzing software tool was launched in all of the following studies. In 2011, accuracy over 84% was achieved with several classification algorithms over

¹ Department of Computer Engineering, Eskişehir Osmangazi University, Eskişehir, Turkey

² Department of Radiology, Eskişehir Osmangazi University, Eskişehir, Turkey

* Corresponding Author: Email: nadar@ogu.edu.tr

Note: This paper has been presented at the 5th International Conference on Advanced Technology & Sciences (ICAT'17) held in Istanbul (Turkey), May 09-12, 2017.

different feature groups comparison using 509 patients within ADNI set [5]. Another study in 2011 classified 524 patients within ADNI set with an accuracy of approximately 89%. There were tests with different classifiers, this ratio was the best value of the support vector machine learning algorithm (SVM) between AD v control subjects [6]. In 2013, Aguilar et al. took the left and the right sides of the brain separately using 345 samples of the AddNeuroMed. The best results of the research were reported as the values between 81.4% and 88.1% in AD v control samples test using miscellaneous classifiers [7]. In 2015, a research applied non-linear SVM to its own dataset of 72 samples. In 3-Class tests, the accuracy results were approximately 70%, and in 2-Class tests, the results were variable between 84.4% and 96.3% [8]. Moreover, 92.4% average accuracy result was reached in a study with SVM using its own dataset formed by combining the data received from different medical centers [9]. In 2016, nearly half of the dataset used in this study was analyzed with artificial neural networks (ANN). Feature groups in different measurements for the left and the right sides of the brain were processed individually, and accuracy results up to 87.5% was gained [10]. In a similar study in 2016, the first phase of the method to be described in this study was applied. The best feature subsets were found for each measurement group and accuracy results up to 93.7% were reported [11]. The best features found in these researches will be discussed with a comparison to our findings in the fourth section. The motivation of this study is determining the set of valuable attributes in different measurements that classify three dementia subtypes with the genetic algorithm based wrapper feature selection (GAWFS) algorithm for the entire brain. This study applies blind search technique to high amount of features, and consists of two main phases resembling the divide and conquer approaches. In the first phase, after the feature extraction step (acquiring numerical data such as cortical volume, thickness, and surface area of the brain sections from Freesurfer brain analyzing software tool), different measurement groups for the left and the right sides of the brain are created. The best feature subsets for all measurement groups are found by applying genetic algorithm (GA) together with various classifiers. In the second phase of the proposed algorithm, the best feature subset search for the entire brain is carried out by merging the feature subsets found in the first phase. The main phases of the blind feature selection from 3D brain models (BFS3D) process flowchart is shown in Fig. 1.

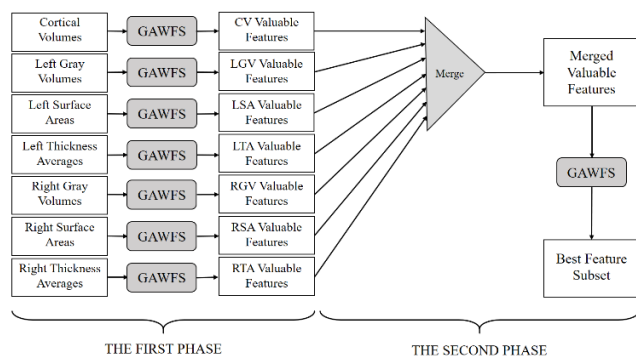


Fig. 1. The main phases of the blind feature selection process

The paper comprises the following. In Section 1, the definition of the dementia diseases, the clinical diagnosis process, and worldwide statistics of dementias are mentioned. In Section 2, the

dataset which the features are extracted from is detailed. In the following section and its subsections, feature extraction, feature selection, classification, and testing methodologies used in this research are expressed. In Section 4, tests and accuracy results are reported statistically, and also the best features classify the dataset are itemized. In the final section, future plans are noticed briefly after the conclusion part.

2. Dataset

The dataset used in this study is shared by the Department of Radiology of Eskişehir Osmangazi University anonymously. The set contains three dementia subtypes (AD, FTD, VaD) over 63 samples. Each individual may be male or female, and can only have one disease. Counts of dementia subtypes over genders are demonstrated in Table 1. Moreover, the minimum encountered age in the dataset is 50 and the maximum is 90.

Table 1. Distribution of dementia subtypes over genders

<i>Dementia Type</i>	<i>Female</i>	<i>Male</i>	<i>All</i>
AD	14	5	19
FTD	13	6	19
VaD	13	12	25
Total	40	23	63

The dataset is a combination of brain imaging studies collected from two different MRI systems having 127.73 or 63.61 imaging frequency between 2014 and 2015. These MRI systems are *Discovery MR750w* (GE, Milwaukee) and *Magnetom Vision plus* (Siemens, Erlangen). Counts of dementia subtypes over MRI systems are demonstrated in Table 2.

Table 2. Distribution of dementia subtypes over MRI systems

<i>Dementia Type</i>	<i>Magnetom Vision plus</i>	<i>Discovery MR750w</i>	<i>All</i>
AD	6	13	19
FTD	6	13	19
VaD	8	17	25
Total	20	43	63

All of the image sets obtained from MRI systems are in version 3 dicom format, grayscale having 12 or 16-bit depth at least 256×256 resolution. Images have MR modality and 2-dimensional MR acquisition type. Slice thicknesses of each T1 sequenced scan are between 4.5 and 5 millimeters. The spacing between slices is variable.

3. Methodology

The methodology of the research is constituted of several sub-steps with two feature selection phases. The flowchart of the sub-steps and the technologies used are shown in Fig. 2. It might be said that some tools have do not support for all operating systems. For this reason, more than one operating system have been installed to working computers, and this issue will be explained in the following subsections.

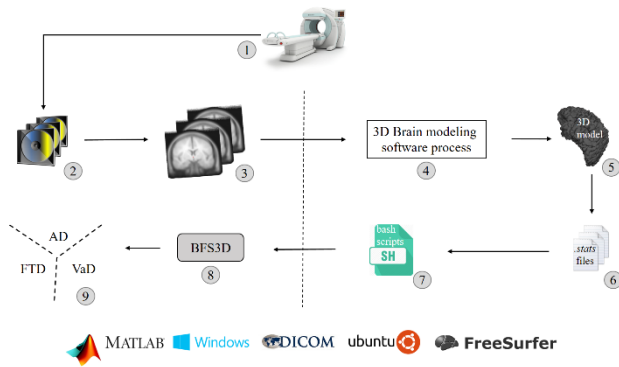


Fig. 2. Blind feature selection methodology

First of all, brain imaging studies are operated in specific MRI systems during clinical investigations. The raw data in compact disks or portable memory units which MRI systems generate as the output of imaging studies is needed to be preprocessed. After analyzing which medical imaging files are appropriate with written programming scripts for the feature extraction process, brains for all samples in the dataset are modeled via the Freesurfer brain analyzing software tool virtually. Besides successful 3D modeling, the measurements of the relevant regions of the brain are expressed also as statistical information. Features of interest are exported from these statistical files using bash scripts. Feature selection process is implemented at the last sub-step of the BFS3D methodology by applying the GAWFS algorithm with various classifiers over two different phases. In the first phase, the sub best attributes within the different attribute groups are calculated. In the second phase, the final results for the entire brain are obtained by bundling partial information coming from the first phase.

3.1. Feature Extraction

Computer assisted medical imaging studies take advantage of some software tools generally. In this study, Freesurfer v5.3.0 brain analyzing and 3D modeling software tool is executed for the purpose of reaching the 3D models over 2D sliced brain image sets. Freesurfer is a program that allows the functional and structural analysis of the human brain. There are several image processing, numerical, etc. sequence of algorithms in the program [12]. The tool can be installed in operating systems such as Unix, Mac OS via open source code. Any user can download this software and its prerequisites from its official site and license it for free. The number of reference documents that explains the use of the software, or that solves encountered errors with unique codes is quite high.

T1 sequenced image sets are implemented as an input to the software tool to model brain in 3D virtually, and to achieve the measurements. First, sliced medical image files are structurally combined with the help of the header details. Then, at the end of the three main cortical reconstruction steps with iterative image processing techniques, the brain is modeled in three-dimension [13]. The essential cascaded sub-steps may be summarized as volumetric registrations, segmentations, visual smoothing transactions, and parcellations [14]. In this research, Freesurfer is set up to a computer that has Intel®Core™ i7-4700 2.40 GHz CPU, 1600 MHz 16 GB RAM, and Ubuntu 14.04 x64 operating system. 3D brain model of each sample is accomplished at between 10 and 15 hours. No manual editing is handled after successful 3D modeling. Statistical files indicating the measurements of the desired brain regions are also acquired as an analysis output such as the 3D model. Those statistics involve volume, thickness, surface area information and also numerical values used in the

calculation of main measurements such as Gaussian curvature, standard deviation, average, minimum, maximum of findings, etc. Linux bash scripts are coded to extract features from certain stat files. From *aseg.stats* files, measurements about segmentation and parcellation anatomy are exported. Likewise, from *lh.aparc.stats* and *rh.aparc.stats* files, characteristics describing gray volumes, surface areas and thickness averages are taken into account. Then, different input matrices are created with combining these numerical expressions. While organizing the matrices, the columns of each matrix are examined separately. Any feature is eliminated from the procedure if there will be no effect at the classification stage. 41 cortical, 34×2 (left and right regions) gray volume, 34×2 surface area and 34×2 thickness average measurements, therefore, 245 features in total are extracted from 3D model. The first phase and hence the second phase are realized using those feature matrices.

3.2. Normalization

The matrix is normalized with the aim of optimizing the effect of each individual attribute in itself before the feature values extracted from 3D models are classified. New values between 0 and 1 for each input feature matrix are generated.

3.3. Feature Selection Using Genetic Algorithm

In classification studies, all the features in the raw feature set may not have a positive effect on correct prediction. Some of them may be insignificant, on the other hand, some may be indispensable. In this respect, it is an important step choosing effective attributes to achieve satisfactory classification findings. In this study, GA is applied as wrapper feature selection algorithm. The basis of the algorithm is the process of evolution from generation to generation. High-quality genes come to the forefront while weak ones are disappearing. Through a fitness function, the algorithm computes a cost or worthiness for the parameters of input vectors namely chromosomes. Chromosomes are constituted from the genes that represent the solution. Each numeric parameter of a chromosome illustrates a different attribute. Chromosomes having the best fitness value are described as worthy input parameters or as valuable attributes. Populations in fixed size manage diverse chromosomes (members) in generation cycles. The purpose of any generation cycle is to estimate the local best solution. The heuristic algorithm eliminates the worst chromosomes, and make significant ones pass to the next level. New generations are built by applying reproduction functions of GA. As creating new generation members, crossover functions that take two parent chromosomes as input, and create new child chromosomes are used. Selection functions determine which chromosomes to consider for these operations. Small changes can be made in some genes by mutation functions randomly. Moreover, chromosomes having better fitness values, namely elites may be placed in next generations straightforwardly. GA process is terminated when stopping criteria is reached, such as minimum fitness tolerance or specified maximum number of generations [15].

ft ₁	ft ₂	ft ₃	ft ₄	ft ₅		bit ₁	bit ₂	bit ₃	bit ₄	bit ₅		ft ₁	ft ₂	ft ₄
0.5	0.316	0.258	0.742	0.316								0.5	0.316	0.742
0.5	0.632	0.258	0.371	0.632								0.5	0.632	0.371
0.5	0.316	0.774	0	0.5		1	1	0	1	0		0.5	0.316	0
0.5	0.632	0.516	0.557	0.5								0.5	0.632	0.557

a. Feature set

b. Chromosome

c. Masked set

Fig. 3. A selection mask example

In this study, the bit string chromosome type indicates which features will be trained and tested by the classifiers. Thus, the chromosomes in the populations behave like selection masks. A

selection mask example is given in Fig. 3. In addition, accuracy result of the classification with selected features is defined as the fitness function. Accordingly, GA was implemented with different parameters inside to find the best feature subset using a wrapper approach. The proposed GAWFS method describing the elimination of the attributes that are not effective during the process is represented in Fig. 4. The input data (Feature Set) and therefore the output data (Valuable Features) differs according to various feature matrices.

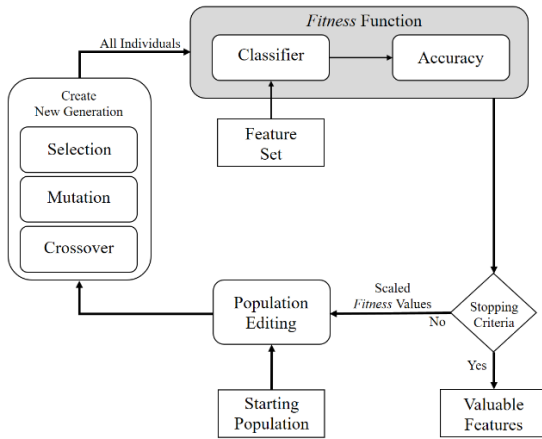


Fig. 4. Genetic algorithm based wrapper feature selection

3.4. Wrapper Classifiers

The GAWFS algorithm is applied with Naive Bayes (NB) and SVM classifiers. NB estimates the conditional probabilities for each class label that predicted sample might be involved. The class label with the maximum probability assigns the class of the unknown sample [16]. Alternatively, the maximum margin classifier SVM separates the hyperplane into two pieces (using kernel functions if necessary) via *one to all* strategy [17].

3.5. Cross Validation Test Technique

k-fold cross validation technique is one of the classification testing methods. Samples in a particular dataset are partitioned into *k* clusters. Respectively, each partition becomes the test set, and the rest implies the train set. Overall performance is calculated by the ratio of correctly predicted clinical diagnoses for whole *k* rounds to all estimates.

The performances of the GAWFS with NB or SVM are computed over applying 10-fold cross validation. Although this work includes different phases, each test uses the same folds within itself. The confusion matrices of different classification tests are achieved by summing the partial prediction results at the end of all folds.

4. Tests and Results

Experimental studies are carried out in two ways using the methods described in the previous sections. 3-Class tests using all classes (AD, FTD, VaD) and 2-Class tests with the "relevant class or not" approach are made. 2-Class tests are initiated by labeling non-relevant samples of the studied class as *others* (Oth).

In the first phase of the tests, the best feature subsets for each feature group are achieved. Following in the second phase, the final worthy set is detected with merging the local sets as illustrated in Fig. 1.

Table 3. Genetic algorithm parameters

Parameter	The 1 st Phase	The 2 nd Phase
Maximum Generation Count	500-1000	1000
Population Size	400-800	800
Elite Count	10%	2.5%
Chromosome Type	Bit String	Bit String
Chromosome Length	Masked Set Length	Masked Set Length
Fitness Scaling Function	Rank	Proportional
Crossover Function	Single Point	Scattered
Crossover Fraction	90%	90%
Selection Function	Roulette Wheel	Roulette Wheel
Mutation Function	Uniform	Uniform
Mutation Rate	13%	13%

During the tests, the parameters given in Table 3 are used. Final results of tests with listed parameters for NB and SVM classifiers are shown in Table 4 and Table 5 respectively.

Table 4. Genetic algorithm based wrapper feature selection results with Naive Bayes classifier

Classes	Feature Count End of Ph1	Best Feat. Subset Count	Acc. %	Confusion Matrix	Best Feat.s
All	103	11	90.5	$\begin{bmatrix} 16 & 1 & 2 \\ 1 & 17 & 1 \\ 0 & 1 & 24 \end{bmatrix}$	NBAll
ADvOth	124	17	93.7	$\begin{bmatrix} 17 & 2 \\ 2 & 42 \end{bmatrix}$	NBAD
FTDvOth	116	17	95.2	$\begin{bmatrix} 17 & 2 \\ 1 & 43 \end{bmatrix}$	NBFTD
VaDvOth	127	10	95.2	$\begin{bmatrix} 23 & 2 \\ 1 & 37 \end{bmatrix}$	NBVaD

- **NBAll**: Cortical volumes: left *putamen*, 4th *ventricle*, left *vessel*, left *choroid-plexus*. Gray volumes: left *bankssts*, left *postcentral*. Surface areas: left *entorhinal*, left *inferiortemporal*, left *isthmuscingulate*, right *middletemporal*, right *supramarginal*.
- **NBAD**: Cortical volumes: left *putamen*, 3rd *ventricle*, left *vessel*, right *cerebellum white matter*. Gray volumes: left *bankssts*, left *medialorbitofrontal*, right *fusiform*, right *rostralmiddlefrontal*. Surface areas: left *posteriorcingulate*, right *caudalanteriorcingulate*, right *postcentral*, right *precuneus*, right *transverse temporal*. Thickness averages: left *posteriorcingulate*, right *inferiortemporal*, right *parahippocampal*, right *insula*.
- **NBFTD**: Cortical volumes: left *vessel*, left *choroid-plexus*, right *caudate*, right *putamen*, right *ventralDC*, 5th *ventricle*. Gray volumes: left *postcentral*, right *medialorbitofrontal*. Surface areas: left *bankssts*, left *paracentral*, left *parstriangularis*, left *precentral*, right *paracentral*. Thickness averages: right *parstriangularis*, right *precuneus*, right *superiorparietal*, right *superiortemporal*.
- **NBVaD**: Cortical volumes: 4th *ventricle*, right *choroid-plexus*. Gray volumes: left *entorhinal*, left *inferiorparietal*, left *isthmuscingulate*, left *postcentral*, left *transverse temporal*, right *supramarginal*. Surface areas: left *cuneus*, right *parahippocampal*.

Table 5. Genetic algorithm based wrapper feature selection results with Support Vector Machines

Classes	Feature Count End of Ph1	Best Feat. Subset Count	Acc. %	Confusion Matrix	Best Feat.s
ADvOth	63	8	92.1	$\begin{bmatrix} 14 & 5 \\ 0 & 44 \end{bmatrix}$	<i>SVMAD</i>
FTDvOth	71	9	90.5	$\begin{bmatrix} 13 & 6 \\ 0 & 44 \end{bmatrix}$	<i>SVMFTD</i>
VaDvOth	73	8	93.7	$\begin{bmatrix} 21 & 4 \\ 0 & 38 \end{bmatrix}$	<i>SVMVaD</i>

- *SVMAD*: Gray volumes: left *bankssts*, left *entorhinal*, left *paracentral*, left *parsopectularis*, right *superiortemporal*. Thickness averages: left *lingual*, *medialorbitofrontal*, right *lingual*.
- *SVMFTD*: Cortical volumes: right *putamen*. Gray volumes: left *fusiform*, left *superiorfrontal*, right *bankssts*, right *inferioparietal*, right *isthmuscingulate*, right *posteriorcingulate*, right *transversetemporal*. Surface areas: right *pericalcarine*.
- *SVMVaD*: Cortical volumes: left *lateral-ventricle*, left *putamen*, right *cerebellum-cortex*, right *pallidum*. Gray volumes: left *parsopectularis*, left *precuneus*, right *caudalanteriorcingulate*. Surface areas: right *precentral*.

Some features are common among the findings obtained in different experimental tests. It is seen that different measurements of *bankssts* and *putamen* regions are encountered in 5 of 7 tests. Likewise in 4 of 7 test outputs, *postcentral* measurements can be observed as valuables. Also, 3 of 7 test findings in a similar manner have different measurements of the regions such as *vessel*, *choroid-plexus*, *entorhinal*, *isthmuscingulate*, *medialorbitofrontal*, *paracentral*, *posteriorcingulate*, *precuneus*, and *transversetemporal*. As a result of these evaluations, *bankssts*, *putamen*, and *postcentral* regions can be evaluated as the most valuable features of this work. The rest may be qualified as the secondary.

When it is desired to interpret each 2-Class test as a subversion of 3-Class tests, findings also support this hypothesis. Except for *middletemporal* region, all the features found as the best ones in 3-Class tests are also included in the 2-Class test results. It might be said that the related region is worthy only in the classification of those three classes.

Some of the brain regions become prominent not in all tests but just in certain 2-Class tests. It is commented that several parts of the brain are more effective in the clinical diagnosis stage of the examined disease. For AD, these measurements are listed as volumes of 3rd *ventricle*, right *cerebellum white matter*; gray volumes of left *medialorbitofrontal*, left *paracentral*, left *parsopectularis*, right *fusiform*, right *rostralmiddlefrontal*, right *superiortemporal*; surface areas of left *posteriorcingulate*, right *caudalanteriorcingulate*, right *precuneus*, right *transversetemporal*; thickness averages of left and right *lingual*, left *medialorbitofrontal*, left *posteriorcingulate*, right *parahippocampal*, right *insula*. For FTD, these measurements are listed as volumes of right *caudate*, right *ventralDC*, 5th *ventricle*; gray volumes of left *fusiform*, left *superiorfrontal*, right *medialorbitofrontal*, right *inferioparietal*, right *posteriorcingulate*, right *transversetemporal*; surface areas of left and right *paracentral*, left *parstriangularis*, left *precentral*, right *pericalcarine*; thickness averages of right *parstriangularis*, right

precuneus, right *superioparietal*, right *superiortemporal*. For VaD, these measurements are listed as volumes of left *lateral ventricle*, right *cerebellum cortex*, *pallidum*; gray volumes of left *inferioparietal*, left *isthmuscingulate*, left *transversetemporal*, left *parsopectularis*, left *precuneus*, right *caudalanteriorcingulate*; surface areas of left *cuneus*, right *parahippocampal*, right *precentral*.

Among the valuable features obtained as a result of 3-Class experimental tests, such brain regions as *entorhinal*, *inferiortemporal*, *middletemporal*, *isthmuscingulate*, and *choroid-plexus* clearly coincide with the findings of some previous studies in the literature [6], [7], [9], [18]. In case the comparison of AD v Oth tests with literature studies that have AD patients in their dataset, *parahippocampal* and *superiortemporal* brain regions are attracting attention as a common [6], [7], [18]. On the other hand, some features, such as *brainstem* and *corpus callosum*, which are considered to be insignificant brain regions in the literature [18], are not found to be valuable too in this research.

5. Conclusion

Methodology criteria are the most crucial factors in obtaining quality findings. The important steps can be listed as image processing algorithms, feature extraction, feature selection, and testing parameters. Also, consistency of study in neuroimaging researches is directly affected by dataset attributes such as sample size, disease subtypes etc.

In this research, blind search technique is followed to detect valuable brain features classify specified dementia subtypes. In the first phase, the most valuable attributes of the several measurements inside the different feature groups are found out. Afterward, the local best sub-attributes found in the previous phase are combined and the final features for the entire brain in different measurements are determined. The valuable attributes found are listed in detail depending on which of the subtypes of the disease is desired to be identified. In the direction of all experimental studies, precious attributes are successfully detected and completely listed by wrapper feature selection algorithm.

The aim of the future studies will be to find more precise results. Standard datasets having a high number of samples, that are internationally recognized, may also be preferred to avoid the overfitting problem altogether. Besides, the results obtained from those datasets are statistically comparable with similar studies in the literature. Additionally, various feature selection and classification algorithms will be used. Statistics will be strengthened with different performance metrics.

References

- [1] C. Güngen, T. Ertan, E. Eker, R. Yaşar, and F. Engin, "Standardize mini mental test'in Türk toplumunda hafif demans tanısında geçerlik ve güvenilirliği," *Türk Psikiyatr. Derg.*, vol. 13, no. 4, pp. 273–281, 2002.
- [2] A. Wimo, B. Winblad, H. Aguero-Torres, and E. von Strauss, "The magnitude of dementia occurrence in the world," *Alzheimer Dis. Assoc. Disord.*, vol. 17, no. 2, pp. 63–67, 2003.
- [3] D. Herek and N. Karabulut, "Manyetik rezonans görüntüleme," *TTD Toraks Cerrahisi Bülteni*, vol. 1, no. 3, pp. 214–222, 2010.
- [4] M. Sebban and R. Nock, "A hybrid filter/wrapper approach of feature selection using information theory," *Pattern Recognit.*, vol. 35, no. 4, pp. 835–846, 2002.
- [5] R. Cuingnet, E. Gerardin, J. Tessieras, G. Auzias, S. Lehericy, M. O. Habert, M. Chupin, H. Benali, O. Colliot, A. D. N. Initiative, and

- others, "Automatic classification of patients with Alzheimer's disease from structural MRI: a comparison of ten methods using the ADNI database," *Neuroimage*, vol. 56, no. 2, pp. 766–781, 2011.
- [6] J. Escudero, J. P. Zajicek, and E. Ifeachor, "Machine Learning classification of MRI features of Alzheimer's disease and mild cognitive impairment subjects to reduce the sample size in clinical trials," in *Engineering in Medicine and Biology Society, EMBC, 2011 Annual International Conference of the IEEE*, 2011, pp. 7957–7960.
- [7] C. Aguilar, E. Westman, J. S. Muehlboeck, P. Mecocci, B. Vellas, M. Tsolaki, I. Kloszewska, H. Soininen, S. Lovestone, C. Spenger, and others, "Different multivariate techniques for automated classification of MRI data in Alzheimer's disease and mild cognitive impairment," *Psychiatry Res. Neuroimaging*, vol. 212, no. 2, pp. 89–98, 2013.
- [8] W. B. Jung, Y. M. Lee, Y. H. Kim, and C. W. Mun, "Automated classification to predict the progression of Alzheimer's disease using whole-brain volumetry and DTI," *Psychiatry Investig.*, vol. 12, no. 1, pp. 92–102, 2015.
- [9] Q. Zhou, M. Goryawala, M. Cabrerizo, J. Wang, W. Barker, D. A. Loewenstein, R. Duara, and M. Adjouadi, "An optimal decisional space for the classification of Alzheimer's disease and mild cognitive impairment," *IEEE Trans. Biomed. Eng.*, vol. 61, no. 8, pp. 2245–2253, 2014.
- [10] S. Okyay, N. Adar, K. Özkan, S. Şaylısoy, D. B. Adapınar, and B. Adapınar, "Classification of some dementia types due to feature selection with artificial neural networks," in *IEEE 24th SIU*, 2016.
- [11] N. Adar, S. Okyay, K. Özkan, S. Şaylısoy, B. D. Özbabalık Adapınar, and B. Adapınar, "Feature Selection on MR Images Using Genetic Algorithm with SVM and Naive Bayes Classifiers," *Int. J. Intell. Syst. Appl. Eng.*, vol. 4, pp. 170–174, 2016.
- [12] B. Fischl, "FreeSurfer," *Neuroimage*, vol. 62, no. 2, pp. 774–781, 2012.
- [13] M. Reuter, N. J. Schmansky, H. D. Rosas, and B. Fischl, "Within-subject template estimation for unbiased longitudinal image analysis," *Neuroimage*, vol. 61, no. 4, pp. 1402–1418, 2012.
- [14] A. M. Dale, B. Fischl, and M. I. Sereno, "Cortical surface-based analysis: I. Segmentation and surface reconstruction," *Neuroimage*, vol. 9, no. 2, pp. 179–194, 1999.
- [15] M. Pei, E. D. Goodman, W. F. Punch, and Y. Ding, "Genetic algorithms for classification and feature extraction," in *Classification Society Conference*, 1995.
- [16] I. Rish, "An empirical study of the naive Bayes classifier," in *IJCAI 2001 workshop on empirical methods in artificial intelligence*, 2001, vol. 3, no. 22, pp. 41–46.
- [17] C. C. J. C. Burges, "A tutorial on support vector machines for pattern recognition," *Data Min. Knowl. Discov.*, vol. 2, no. 2, pp. 121–167, 1998.
- [18] E. Westman, A. Simmons, J. S. Muehlboeck, P. Mecocci, B. Vellas, M. Tsolaki, I. Kloszewska, H. Soininen, M. W. Weiner, S. Lovestone, and others, "AddNeuroMed and ADNI: similar patterns of Alzheimer's atrophy and automated MRI classification accuracy in Europe and North America," *Neuroimage*, vol. 58, no. 3, pp. 818–828, 2011.